New type of Y-branch power splitter and beam expander based on eliminating anomalous reflection effect

Jian Sun (孙 建)[1], Yifeng Shen (沈义峰)[1,3*], Juan Wang (王 娟)[1], Lulu Sun (孙露露)[1], Kui Han (韩 奎)[1], Gang Tang (唐 刚)[1], and Guozhong Wang (王国中)[2,3]

[1]*Department of Physics, China University of Mining and Technology, Xuzhou 221008*

[2]*School of Physics and Telecommunication, Wenzhou University, Wenzhou 325035*

[3]*State Key Laboratory of Functional Materials for Informatics, Shanghai Institute of Microsystem and Information Technology, Chinese Academy of Sciences, Shanghai 200050*

[*]*E-mail: shen_syf@163.com*

Received June 18, 2008

We propose a new type of Y-branch power splitter and beam expander with scales of microns in two-dimensional (2D) photonic crystals (PCs) by drilling air holes in a silicon slice. Its functionality and performance are numerically investigated and simulated by finite-difference time-domain (FDTD) method. Simulation results show that the splitter can split a TE polarized light beam into two parallel sub-beams and the distance between them is tunable by changing the parameters of the splitter, while the expander can expand a narrow beam into a wider one, which is realized in an integrated optical circuit. The proposed device is based on the avoiding of anomalous reflection effect and the coupling transmission of defect modes of the interfaces.

OCIS codes: 350.4238, 230.1360, 120.1680.

doi: 10.3788/COL20090703.0251.

Photonic crystals (PCs) are artificial materials that have periodic dielectric structures. Due to their unique ability to modify photon interaction with host materials by projecting special structure of material, nowadays PCs have become an active research area[1−3]. It is very astonishing that a beam of electromagnetic wave could propagate almost without diffraction in perfect PCs, which is called self-collimation and has attracted much attention[4−7]. The phenomena associated with PCs, such as super prism, anomalous reflection, and negative refraction, have been observed in experiments[8−10]. Yu *et al.* have shown that for a self-guiding beam incident upon the interface of PCs from a uniform dielectric, the direction of the reflected beam is independent of the orientation of the interface within certain incident angle range, which is called the anomalous reflection[9]. The principles of self-collimation and anomalous reflection have been employed in the new type of optical apparatus[11−14].

In this letter, we investigate a two-dimensional (2D) square lattice PC composed of air holes in a silicon slice. Using the equal-frequency contours (EFCs), we analyze the anomalous reflection and self-collimation phenomena for this structure. To avoid the anomalous reflection effect, a triangular area is properly etched in the PC. The etched area plays a role of a power splitter or a beam expander for an incident beam with a TE polarization[15] (the electric field is perpendicular to the axis of the air holes), as confirmed by the finite-difference time-domain (FDTD) simulations[16]. The physical mechanism of the beam expander is also discussed. We found that the truncation of the interface between the etched area and the PC is very important for beam transmission because of the coupling of the defect modes[11].

For general dielectrics, the reflection of a light beam is governed by the well-known Snell's law, which states that the reflection angle of light beam is strictly equal to its angle of incidence. However, for PCs, the direction of energy flow is determined by $\vec{v}_{\rm g} = \nabla_{\mathbf{k}}\omega$[8], where $\vec{v}_{\rm g}$ is the group velocity, $\mathbf{k}$ is the wave vector, and ω is the angular frequency. The complex band structures lead to a great difference such that the energy flow can propagate along other directions rather than that of the wave vector $\mathbf{k}$. So the reflection of a light beam upon the interface between PCs and a uniform dielectric is not necessary to satisfy Snell's law, and the anomalous reflection can take place.

In order to determine the conditions for anomalous reflection taking place, we performed the EFC analysis for the reflection behavior. We only consider the condition that a light beam is incident from the PC structure to a homogenous dielectric (for example air). The PC structure considered in this letter is shown in the inset of Fig. 1, which consists of a $(44\sqrt{2}a \times 19\sqrt{2}a)$ square

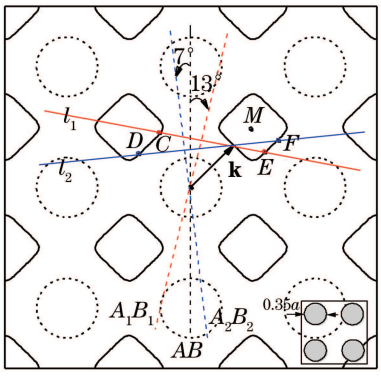

Fig. 1. EFC for the PC structure shown in the inset is formed by a square lattice of air holes in a silicon slice. The solid square-like lines represent the contours for the PC structure for frequency $0.19c/a$, and the dashed circles are the EFC for air for the same frequency.

lattice of air holes with the air-hole radius of $0.35a$ (a is the lattice constant) introduced in a silicon slab (the refractive index $n = 3.5$). Only along the ΓM direction, self-collimation can take place[17]. For a self-collimated beam with a wave vector $\mathbf{k}$ propagating along the ΓM direction, if the incident interface (the PC-air interface) is chosen as the (10) plane (the dashed line AB in Fig. 1 represents the cross line between the (10) plane and the EFC section), the reflected beam will have a 90° bend since the incident angle is 45°. As the orientation of the incident interface rotates about an axis perpendicular to the EFC section through the Γ point and deviates a small angle from the (10) plane, the reflected beam will still remain a 90° bend, which is referring to the anomalous reflection. From the EFC calculations, we can determine the range of the orientation of the incident interface deviating from that of the (10) plane, within which the reflection angle largely remains unchanged. When we vary the orientation of the incident interface from the orientation of AB (the (10) plane) to that of A_1B_1 (A_1B_1 denotes the cross line of the incident interface with the EFC section), one can draw a "**k**-conservation" line l_1 through the head of the incident wave vector $\mathbf{k}$ in a direction perpendicular to A_1B_1, which intersects the EFC of PC structure at point C in the first Brillouin zone. From Fig. 1, we can get the critical angle for A_1B_1 relative to AB in the clockwise direction by geometrical solution, which is found to be about 13°. If the angle between the incident interface and the (10) plane in the clockwise direction exceeds this critical angle, the "**k**-conservation" line l_1 would not intersect with the EFC of PC structure at the linear part of each side or even has no intersection in the first Brillouin zone except the arrowhead of the wave vector. Therefore, no anomalous reflection can take place anymore. Similarly, we can determine the critical angle in counterclockwise direction, namely the maximal angle between AB and A_2B_2, which is about 7°. The magnitude of these two angles is consistent with the FDTD simulation results. Consequently, the orientation of the incident interface can be truncated along the direction in a 20° angle range between A_1B_1 and A_2B_2 for anomalous reflections taking place. If we gradually increase the angle between the incident interface and the (10) plane in counterclockwise direction to exceed the critical angle of 7°, the "**k**-conservation" line will no longer intersect with the EFC of the PC structure at the first Brillouin zone except the arrowhead of the wave vector, but intersect with the EFC at the second Brillouin zone. As a result, the anomalous reflection would be greatly depressed corresponding to an increase of the transmission. In the light of the preceding analysis, we can design a power splitter and a beam expander.

In Fig. 2, we establish an orthogonal coordinate system in the PC, in which the x axis is along the ΓM direction, and the origin is at the center of an air hole. If the isosceles triangular part in Fig. 2 is etched away, then the PC system becomes a beam splitter, which means that it can split one beam into two parallel sub-beams. To be explicit, the beam splitter (expander) denotes the whole PC system, which involves two parts: the self-guiding region and the splitting region (the triangular air area). The parameters of splitter (expander) only concern that of the isosceles triangle air part. As shown in Fig. 2, the

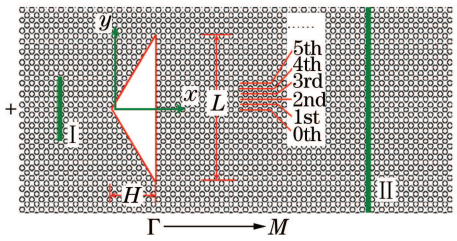

Fig. 2. Silicon background of the isosceles triangle region is etched away, and the whole PC structure becomes a beam splitter. The symbol "+" indicates a continuous Gaussian light source. The two wide vertical lines I and II represent two power monitors.

vertex of the splitter is fixed at the point $(-0.3a, 0)$, the length of hemline L is $20a$ and is kept unchanged for the convenience of discussion, while the height H is allowed to vary from $6.1a$ to $7.6a$. Choosing $-0.3a$ as the x coordinate of the splitter vertex is only because $-0.3a$ is the optimum value to obtain the maximum transmission of light beam by parameter scanning in FDTD simulations. Here, the process of fixing the length L and changing the height H is just equivalent to that of fixing the height H and changing the length L, because the significant variable parameter is the vertex angle of the splitter $\theta = 2\arctan(L/2H)$. These parameters of splitter are chosen for an incident beam with a width of $4a$ and the beam width also stays constant in the context. The vertex angle of the triangular air area varies with different splitter heights H due to a fixed hemline length L, so the incident angle of the self-collimated beam propagating along the x axis can be controlled by designing appropriate values of splitter height H.

In Fig. 2, a continuous Gaussian beam source with a beam width $4a$ and the working frequency $0.19c/a$ is placed at $(-14.5a, 0)$. Two power monitors (I and II) are located at $(-8a, 0)$ and $(37a, 0)$, respectively, by which one can obtain the power intensity and the field distribution of the beam along the y direction. The widths of two monitors along the y direction are $6\sqrt{2}a$ and $19\sqrt{2}a$, which are large enough to measure the power of the corresponding beams. The perfectly matched layer (PML) absorbing boundary conditions are used at the boundary of PC.

We performed the FDTD simulation and obtained the steady-field pattern (z component of the magnetic field) for the splitter of height $7a$, as shown in Fig. 3. An incident beam with a width $4a$ propagating from left to right along the ΓM direction through the PC-air interface of the isosceles triangle air part is separated into two collimated beams with nearly the same widths. The separated distance between two beams is about $8.1a$, and each beam exhibits self-collimation characteristic along

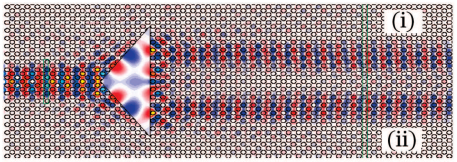

Fig. 3. Steady-field pattern obtained by FDTD simulation at the splitter height $H = 7a$. The width of the incident beam is $4a$. The symbols (i) and (ii) represent the up-beam and the down-beam, respectively.

the ΓM direction. Therefore, this device can be regarded as a genuine beam splitter. There is a small part of power dissipation occurring at the incident interfaces due to reflections. The transmission is defined as the ratio of the average outgoing energy flow to the incident energy flow. The total transmission is about 67% for the configuration described above.

We define the separated distance D of two parallel beams as the spatial distance of their power intensity maxima, so we should firstly determine the center point of the beam. Based on the power intensity distribution measured by the power monitor II, we can theoretically get the distance D, which varies with the height H of the splitter and can be expressed as

$$D = \frac{\int_{-\infty}^{\infty} y|H_{1z}|^2 \mathrm{d}y}{\int_{-\infty}^{\infty} |H_{1z}|^2 \mathrm{d}y} - \frac{\int_{-\infty}^{\infty} y|H_{2z}|^2 \mathrm{d}y}{\int_{-\infty}^{\infty} |H_{2z}|^2 \mathrm{d}y}, \quad (1)$$

where H_{1z} and H_{2z} indicate the magnetic fields of the beam (i) and beam (ii). However, the steady-field distributions of the two separated parallel beams overlap with each other. In fact, it is impossible to distinguish H_{1z} and H_{2z} from the power distribution measured by the power monitor II. As a result, Eq. (1) cannot be used to calculate the distance of two separated beams. We utilize the Gaussian functions to fit the power intensity distribution only in the upper half space $y \geq 0$, and find out the center of the upper beam (i). Because two separated beams are completely the same in the upper and lower spaces, once the center of one beam is determined, the other is also known. Therefore the distance D of two separated beams is determined.

We assume that all other concerned parameters remain fixed, and only the height H of the isosceles triangular air part is allowed to vary from $6.5a$ to $7.6a$. The distance D between two separated beams monotonically increases with the height of the splitter, as shown in Fig. 4. It has an approximate proportional relation with the height H. When the height of the splitter is $7.6a$, the vertex angle of splitter is $2 \times 53°$. The incident interface deviates from the (10) plane with an angle of $53° - 45° = 8°$, which has exceeded the maximal angle 7° of the "**k**-conservation" line l_1 intersecting with the EFC at the first Brillouin zone in counterclockwise direction. The "**k**-conservation" line perpendicular to the incident interface would intersect with the EFC for the air, which means more energy flow can get into the air and the anomalous reflection would be greatly depressed. We define the air holes which intersect with the x axis as the zeroth order air holes, and the other rows of air hole can be classified as the 1st, 2nd, 3rd, $\cdots$ orders in the upper space (see Fig. 2). When the height of splitter is $7.6a$, the incident interface firstly truncates one 5th order air hole $(\frac{3\sqrt{2}}{2}a, \frac{5\sqrt{2}}{2}a)$. So the incident interface is generally of air hole defects and not a perfect plane. When the height of splitter is $6.5a$ (the vertex angle of splitter is $2 \times 57°$), the incident interface of splitter first truncates a 3rd order air hole $(\frac{\sqrt{2}}{2}a, \frac{3\sqrt{2}}{2}a)$, and the distance between the two separated beams decreases too. In the limit of this procedure, the two separated beams can overlap with each other or even merge into one beam. The analysis above shows that by eliminating the anomalous reflection effect, more power will couple into the air splitter. Actually, the physical mechanism of the splitting device is that the splitting effect comes from the refraction (away from the beam center) of the beam by the interface between PCs and a uniform medium. The function of the right-hand side part of the splitter is to collimate the propagation along ΓM direction. The two outgoing beams of the splitter could overlap and merge into one wider self-collimated beam. The critical condition of the splitter for one incident beam being separated into two distinct beams or still keeping one beam is that whether the y coordinate of the first air hole defect is larger than $\frac{3\sqrt{2}}{2}a$ or not. This critical condition is nevertheless empirical obtained by the simulation process.

Figure 5 shows the sum of power intensities of two separated beams versus the height of splitter with the splitter vertex fixed at $(-0.3a, 0)$. The power intensity normalized with that of the incident beam can be obtained by using the power monitors. The transmitted power intensity remains above 60% in the whole scanning range. Especially in the range $(6.6a, 6.8a)$, the power intensity is over 90%. This is due to the fact that with the height of splitter decreasing, the incident interface gradually deviates from the (10) plane in the counterclockwise direction and the anomalous reflection effect is greatly depressed, so the transmitted beams become stronger.

We note that the distance of the two parallel separated beams decreases with the height of splitter (Fig. 4). When the height of splitter decreases to $6.5a$, the incident interface of splitter first truncates one 3rd order air hole, and two separated beams merge into a wider

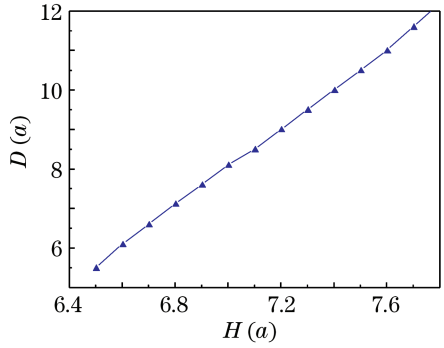

Fig. 4. Distance between the two separated beams D versus splitter height H. The vertex of the splitter is fixed at $(-0.3a, 0)$.

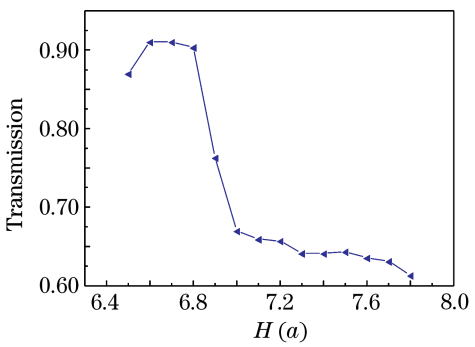

Fig. 5. Power intensity of the transmitted beams varies with the height of splitter H as the vertex of power splitter is located at $(-0.3a, 0)$.

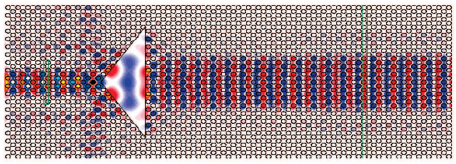

Fig. 6. Steady-field pattern obtained by FDTD simulation. The width $4a$ of the incident beam is expanded to $7.6a$.

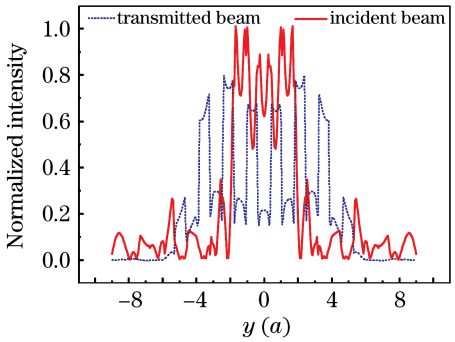

Fig. 7. Beam profiles for the case of Fig. 6.

beam. When the height of splitter decreases continuously to $6.4a$, the incident interface will have more micro defects. The incident beam will couple into the splitter through the channels of micro defects. The two separated beams overlap to form a wider beam. In other words, the device now becomes a beam expander when the height of splitter is $6.4a$.

Figure 6 shows the steady-field pattern by the FDTD simulation for the situation that the incident beam with a width of $4a$ is expanded into one wider beam with a width of $7.6a$, which is 1.9 times of that of the incident beam. The profiles for the field intensity of the expanded beam are very similar to that of the incident beam, which is shown in Fig. 7. Due to the back reflection, a small part of power dissipation occurs at the incident interfaces. The reflection can be illustrated by the EFC in Fig. 1. The **k**-conservation Line l_2 intersects with the EFC of the PC at point E of the second Brillouin zone, which can induce weak reflection. The transmitted energy flow exceeds 76% despite the fact that there are more power reflected back into PC at the incident interface. When the height of beam expander continuously decreases from $6.4a$ to $6.1a$, the incident beam will have more air hole defects to couple into the isosceles triangular air part, and the two separated beams will overlap gradually, leading to the beam width getting smaller in this process. When the splitter height H is $6.1a$, the transmitted beam has almost the same width as that of the incident beam and the device only changes the power intensity distribution of the beam just like an attenuator.

In summary, by suppressing the anomalous reflection effect, the proposed device can split one incident beam into two parallel separated sub-beams. When the incident interface of the splitter intersects through one of the 3rd order air holes, the two separated beams can overlap and become one wider beam. The condition for this device being a beam splitter or a beam expander is determined by the y coordinate of the first truncated air hole of the incident interface. When this value is less than $\frac{3\sqrt{2}}{2}a$, the device is a beam splitter, otherwise a beam expander. To our knowledge, this is the first time to propose a beam expander in an integrated optical circuit, which has many advantages over the conventional ones, for example, the beam expander is compact and easily produced, while the lens combination is hardly integrated into optical circuit to expand a beam. By changing the height of the splitter, it is easy to satisfy the various requests and guarantee a high transmission. Although we only consider the 2D PC system which has an infinite length along the vertical direction, it is reasonable for a basic PC slab structure of air rods embedded in a solid silicon background. In such structures, light can be confined in the third dimension by traditional index guiding. So the proposed device may have much potential application in fiber communication and integrated optical circuits.

This work was supported in part by the Science Foundation of China University of Mining and Technology under Grant No. OK061065.

References

1. E. Yablonovich, Phys. Rev. Lett. **58,** 2059 (1987).
2. S. John, Phys. Rev. Lett. **58,** 2486 (1987).
3. Y. Zhao, Y. Zhang, and B. Li, Chin. Opt. Lett. **3,** S196 (2005).
4. H. Kosaka, T. Kawashima, A. Tomita, M. Notomi, T. Tamamura, T. Sato, and S. Kawakami, Appl. Phys. Lett. **74,** 1212 (1999).
5. J. Witzens, M. Lončar, and A. Scherer, IEEE J. Sel. Top. Quantum Electron. **8,** 1246 (2002).
6. D. N. Chigrin, S. Enoch, C. M. S. Torres, and G. Tayeb, Opt. Express **11,** 1203 (2003).
7. X. Yu and S. Fan, Appl. Phys. Lett. **83,** 3251 (2003).
8. H. Kosaka, T. Kawashima, A. Tomita, M. Notomi, T. Tamamura, T. Sato, and S. Kawakami, Phys. Rev. B **58,** R10096 (1998).
9. X. Yu and S. Fan, Phys. Rev. E **70,** 055601 (2004).
10. M. Notomi, Phys. Rev. B **62,** 10696 (2000).
11. D. M. Pustai, S. Shi, C. Chen, A. Sharkawy, and D. W. Prather, Opt. Express **12,** 1823 (2004).
12. W. Y. Liang, J. W. Dong, and H. Z. Wang, Opt. Express **15,** 1234 (2007).
13. D. W. Prather, S. Shi, J. Murakowski, G. J. Schneider, A. Sharkawy, C. Chen, B. Miao, and R. Martin, J. Phys. D **40,** 2635 (2007).
14. Y. Shen, J. Sun, X. Shen, J. Wang, L. Sun, K. Han, and G. Wang, Chin. Opt. Lett. **6,** 709 (2008).
15. J. D. Joannopoulous, S. G. Johnson, J. N. Winn, and R. D. Meade, *Photonic Crystals: Molding the Flow of Light* (2nd edn.) (Princeton University Press, Princeton, 2008) p.67.
16. A. Taflove, *Computational Electrodynamics: the Finite-Difference Time-Domain Method* (Artech House, Boston, 1995) p.36.
17. C. Luo, S. G. Johnson, J. D. Joannopoulos, and J. B. Pendry, Phys. Rev. B **65,** 201104 (2002).